SUPPLEMENTARY INFORMATION

India-Asia collision was at 24°N and 50 Ma: palaeomagnetic proof from southernmost Asia

Jun Meng[1] Chengshan Wang[1]* Xixi Zhao[2] Rob Coe[2] Yalin Li[1] David Finn[2]

1 State Key Laboratory of Biogeology and Environmental Geology (China University of Geosciences), Beijing 100083, China

2 Department of Earth and Planetary Sciences, University of California, Santa Cruz, CA 95064, USA

*Corresponding author: chshwang@cugb.edu.cn

First author: mj.chen2009@gmail.com

Supplementary Figures

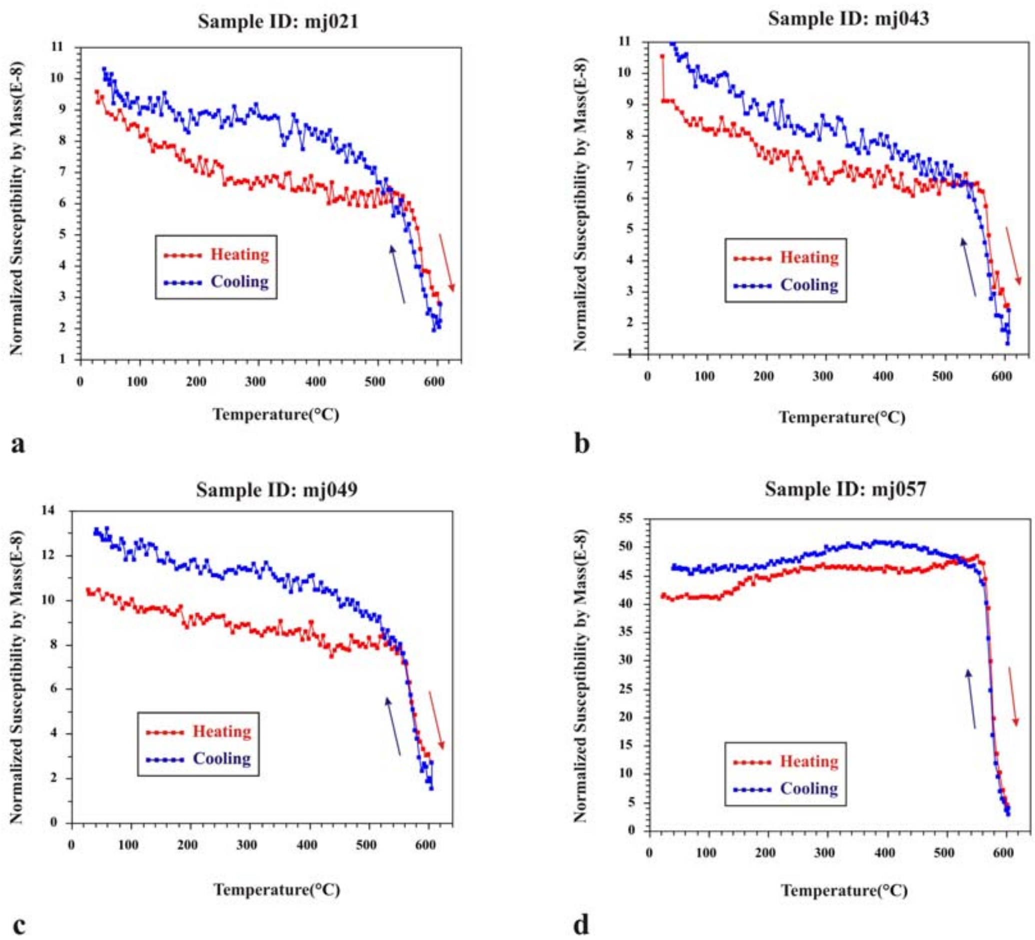

Fig. S1 Normalized susceptibility by mass vs. temperature. All samples heated in an argon environment.

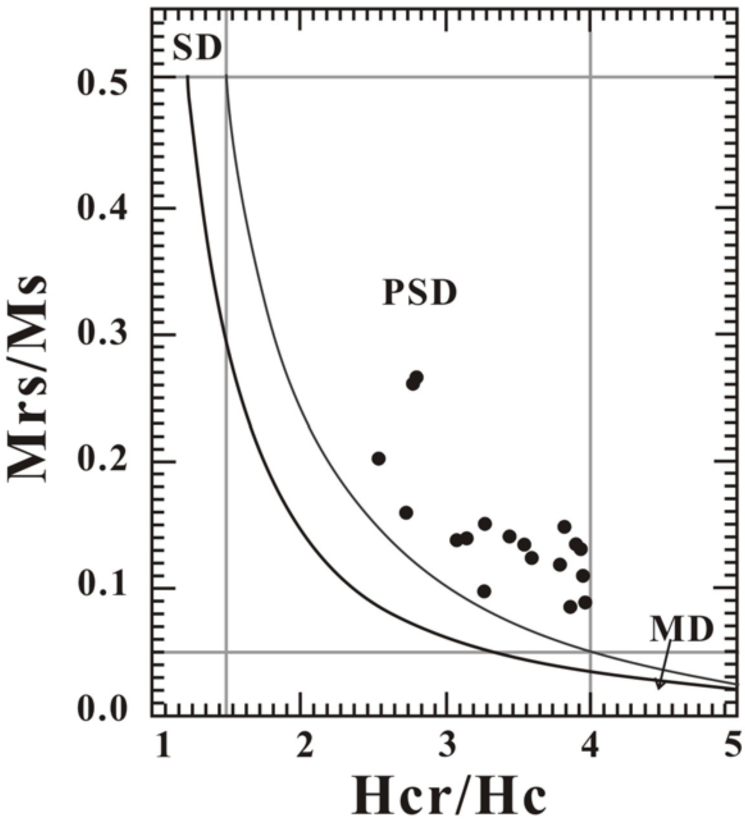

Fig. S2 Day plot[1] of hysteresis data, showing the magnetic grain size of samples. The straight grey lines mean magnetic grain size fields: single-domain (SD), pseudo-single domain (PSD) and multidomain (MD). Thick curved solid line is a theoretical mixing curve of MD and uniaxial single-domain (SD) magnetite; thin curved line is a mixing curve of MD and cubic SD magnetite[2].

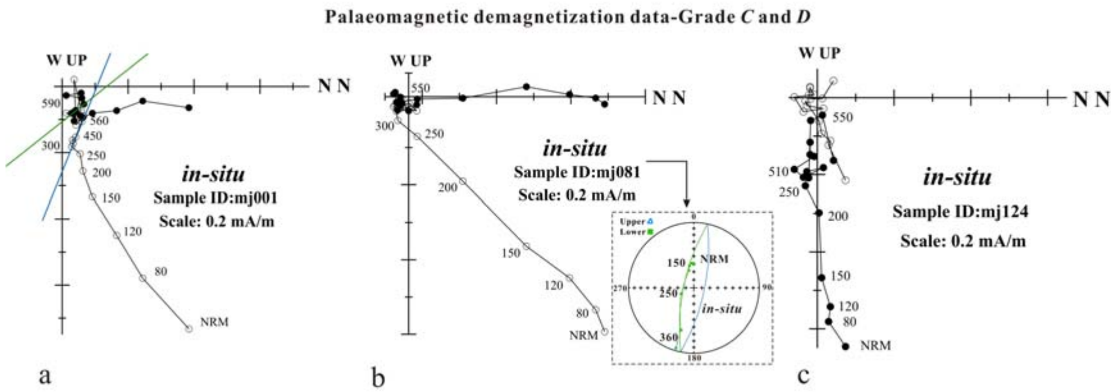

Fig. S3 Representative orthogonal projections of grades *C* and *D* palaeomagnetic demagnetization data from upper Cuojiangding Group plotted in *in-situ* coordinate. Solid (open) circles are the horizontal (vertical) plane projections. Scales are in mA/m. Green and blue straight lines represent the least-square-best fitting directions of the ChRM. Green and blue circle indicate the NRM directions distributed along with the great circle in the equal-area projection. See text for description of demagnetization behavior.

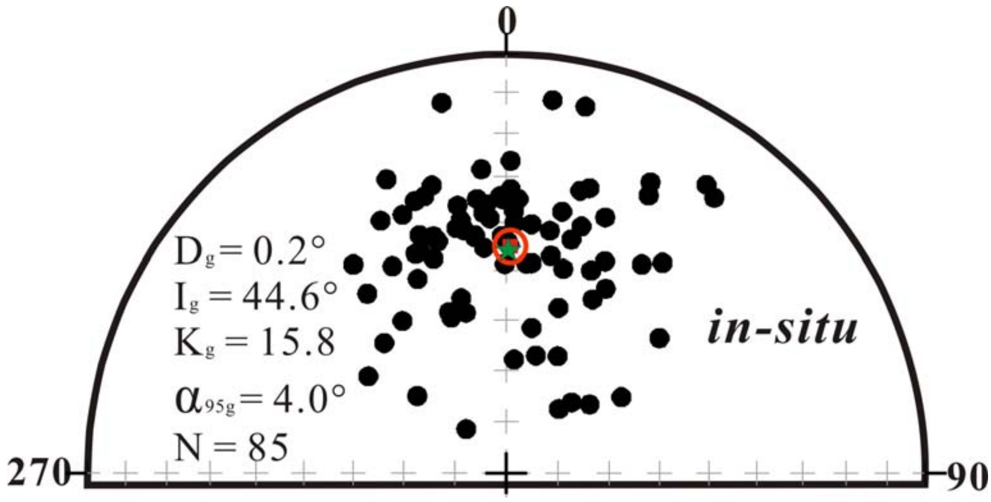

Fig. S4 Equal-area projections of *in-situ* site mean direction for the low temperature component (LTC) from upper Cuojiangding Group. Solid black circles indicate lower hemisphere projections. Solid red square stands for the site mean direction. Green star presents local geomagnetic field.

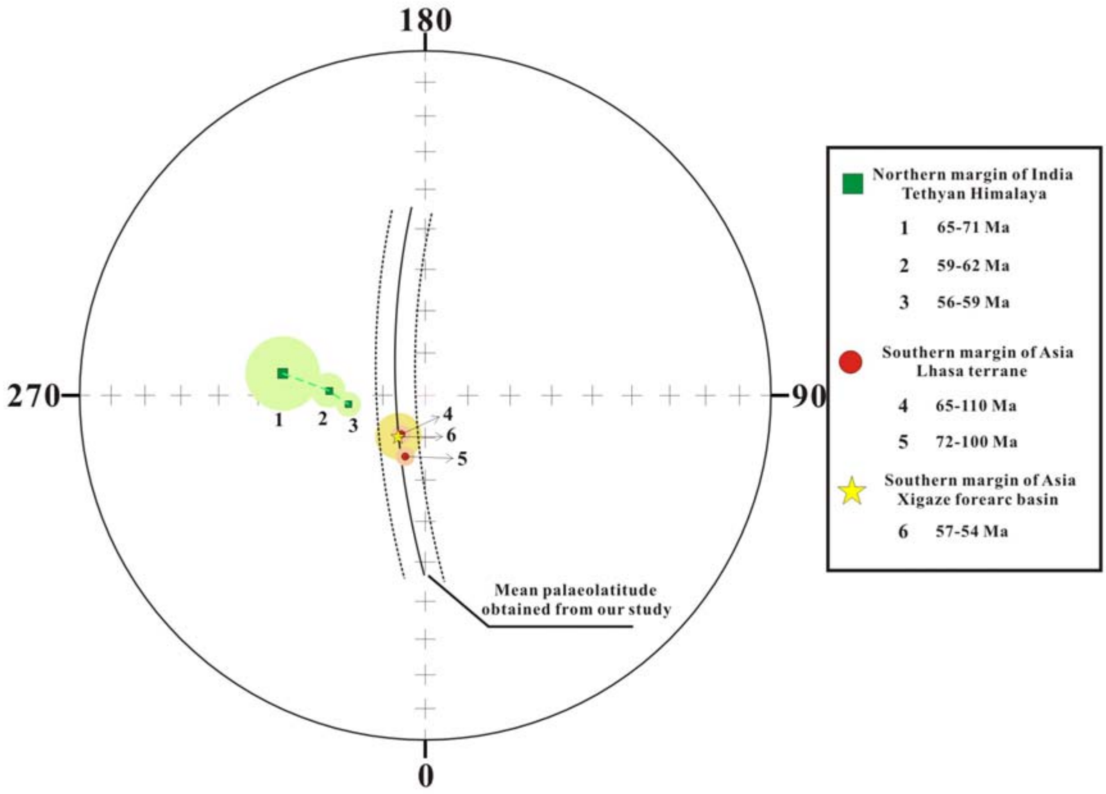

Fig. S5 Equal-area projection showing palaeomagnetic poles of a reference site comparison between northern margin of India and southern margin of Asia. Numbers 1-6 correspond to palaeomagnetic poles described by the authors as follows: 1, Patzelt *et al.* (1996)[3]; 2 and 3, Yi *et al.* (2011)[4]; 4, Tan *et al.* (2010)[5]; 5, Sun *et al.* (2012)[6] and van Hinsbergen *et al.* (2012)[7]; 6, This study. The black line stands for the palaeolatitude obtained from the upper Cuojiangding Group. Confidence limits which were calculated according Coe *et al.* (1985)[8] are illustrated as black dashed lines. The data are plotted in the Northern Hemisphere. All the selected results from Asia are indistinguishable within the error, indicating a constant palaeolatitude for the southern margin of Asia from the Cretaceous to Palaeogene time.

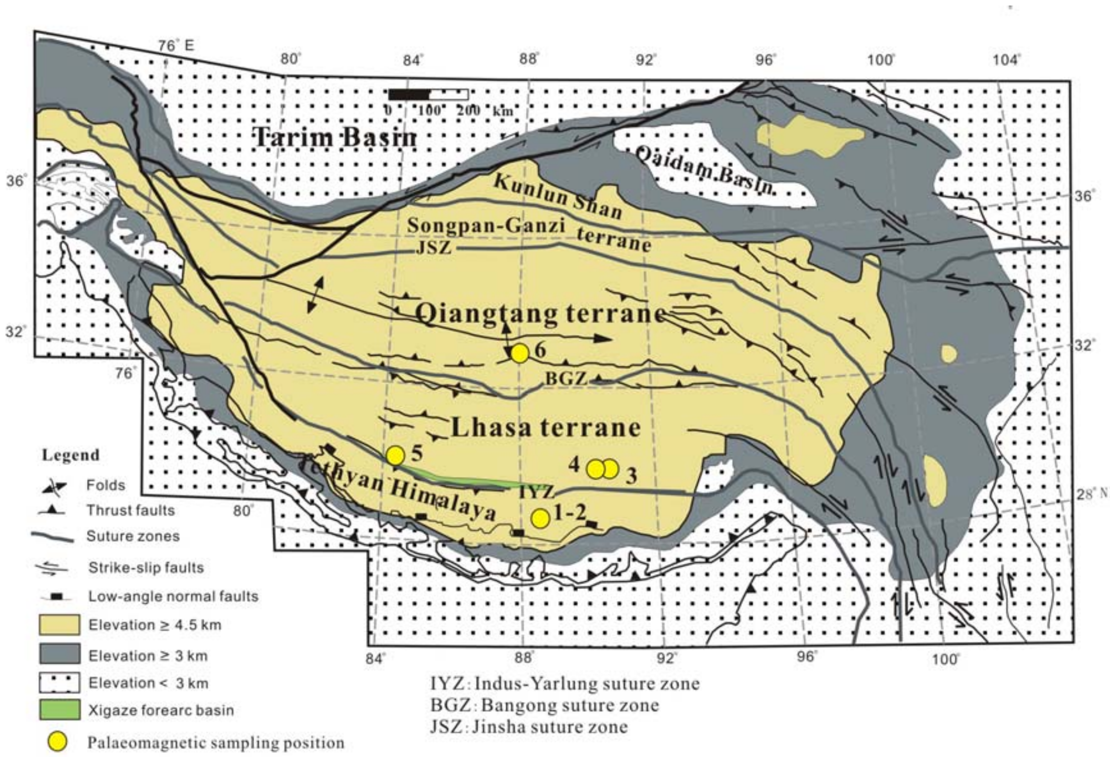

Fig. S6 Tectonic and topographic map of the Tibetan-Himalaya to show the sampling locations of palaeomagnetic studies we used for this study (Modified after DeCelles *et al.* 2007[9]). Numbers 1-6 correspond to palaeomagnetic studies as follows: 1, Patzelt *et al.* (1996)[3]; 2, Yi *et al.* (2011)[4]; 3, Tan *et al.* (2010)[5]; 4, Sun *et al.* (2012)[6] and van Hinsbergen *et al.* (2012)[7]; 5, This study; 6 Lippert *et al.* (2011)[10].

Supplementary Tables

Table S1: Sample characteristic remanent directions (ChRMs) for the upper Cuojiangding Group

Site ID	Strike	Dip	Direction fit code	Demagnetization steps	N	Dg	Ig	Ds	Is	α95s	Grade	Used or not
				Quxia Formation								
mj001	65	84	Dir PCA	T330-T450	4	139.2	64.3	147.9	-18.7	13.7	C	no
mj002	65	84	DirOPCA	T330-T590	10	197.3	37.2	194	-31.5	6.8	A	yes
mj004	65	84	Dir PCA	T330-T450	4	176.1	69	162.6	-13.6	8.9	B	yes
mj005	65	84	Dir PCA	T360-T530	5	95.4	80.9	147.2	-1.4	6.8	B	yes
mj006	65	84	DirOPCA	T360-T500	4	171	61.8	163	-21.1	8.2	B	yes
mj007a	65	84	Dir PCA	T360-T450	3	221.4	30.6	210.5	-16.9	13.1	C	no
mj008a	65	84	Dir PCA	T250-T450	6	77.5	72.4	137.8	-2	9	C	no
mj017	90	65	DirOPCA	T450-T670	12	174.9	18.7	173.1	-46	6.4	A	yes
mj018	90	65	Dir PCA	T330-T530	6	126.2	35.4	137.9	-11.1	10.7	B	yes
mj019B	90	65	DirOPCA	T330-T580	9	145.7	29.1	146.6	-26.7	15.2	A	yes
mj020	90	65	DirOPCA	T450-T580	6	200.7	-13.4	243.2	-67.3	7.3	A	yes

mj021	90	65	Dir PCA	T360-T590	9	186.9	47.4	184.9	-17.3	7.6	A	yes
mj023-1	90	65	DirOPCA	T450-T580	6	164.3	22.3	160.9	-40.3	14.2	B	yes
mj023	90	65	DirOPCA	M030-M070	5	177.7	18.2	176.9	-46.7	4.1	A	yes
mj025	90	65	Dir PCA	T570-T590	3	156.1	39.6	160.4	-21.6	2.2	A	yes
mj026	90	65	Dir PCA	T330-T450	4	181.1	26.9	181.2	-38	18.9	C	no
mj036	90	65	DirOPCA	T640-T690	4	145.2	31.6	147.8	-24.3	4.1	B	yes
mj038	90	65	Dir PCA	T390-T590	8	149.3	6.5	132.4	-46.6	7.3	A	yes
mj039	90	65	DirOPCA	T420-T590	15	147.5	12.4	136	-40.9	9.3	B	yes
mj040	90	65	Dir PCA	T480-T530	4	171.1	2.7	161.5	-61	12.8	B	yes
mj041	90	65	DirOPCA	T360-T590	9	174.9	36.6	175.4	-28.2	7.1	A	yes
mj042	90	65	Dir PCA	T420-T480	3	201.6	22.2	205.8	-38.3	12.2	B	yes
					Gyalaze Formation							
mj043	90	65	DirOPCA	T300-T600	20	152.3	4.3	133.6	-50.2	5.3	A	yes
mj044	90	65	DirOPCA	T390-T580	15	191	32.9	190.8	-31.2	12.7	A	yes
mj045	90	65	DirOPCA	T480-T590	13	194.1	-8.8	222.1	-68.9	7.3	A	yes
mj046	90	65	DirOPCA	T420-T600	16	166.5	-2.2	148	-63.8	9.4	A	yes

mj047	90	65	Dir PCA	T330-T450	5	179.7	51.8	179.8	-13.2	7.7	B	yes
mj048	90	65	DirOPCA	T570-T600	5	129.5	25.5	132.3	-19.8	13.9	C	no
mj049	90	65	DirOPCA	T530-T570	7	190.9	33.8	190.5	-30.3	8.9	A	yes
mj050	90	65	DirOPCA	T250-T640	15	2.4	10.5	9.3	75.3	11.8	C	no
mj051	90	65	DirOPCA	T300-T550	12	183.3	-25.5	280.7	-87	6.2	B	yes
mj052	90	65	Dir PCA	T540-T560	3	60.7	-26.4	53	12.1	1.6	C	no
mj053	90	65	Dir PCA	T520-T575	9	147.1	10.1	133.6	-42.5	7.2	B	yes
mj054	90	65	DirOPCA	T300-T565	15	150.4	33.4	152.9	-25.1	9.6	A	yes
mj055-1	94	74	DirOPCA	M020-M060	5	179.3	36.5	179.3	-37.3	2.9	A	yes
mj055	94	74	DirOPCA	T500-T570	4	173.6	4.4	156.3	-67.1	11.4	A	yes
mj056	94	74	DirOPCA	T480-T580	10	171	4.1	150.4	-66.1	6.9	A	yes
mj057	94	74	DirOPCA	T480-T565	9	203.6	49.4	197.7	-22.3	2.6	A	yes
mj058	94	74	Dir PCA	T510-T530	3	197	8.2	212.9	-62.6	14.3	B	yes
mj059	94	74	Dir PCA	T450-T590	7	121.7	43	143.2	-7.9	9.5	B	yes
mj060	94	74	Dir PCA	T480-T530	4	144	54.8	161.8	-11.5	14.1	C	no
mj061	94	74	DirOPCA	T420-T565	11	229.6	17.9	238.9	-33.7	7.2	B	yes

mj063	94	74	DirOPCA	T510-T570	10	163.6	60.5	173.9	-11.8	9.2	B	yes
mj065	94	74	DirOPCA	T520-T580	10	137.1	55.9	159.6	-8.1	6.3	A	yes
mj066	94	74	Dir PCA	T330-T480	6	148	47.7	159.3	-18.6	7.7	A	yes
mj067	92	74	Dir PCA	T250-T390	5	241.3	15.7	246.4	-23.4	11.8	C	no
mj068	92	74	DirOPCA	T510-T590	9	357	-7.9	349.8	65.6	1.6	A	no
mj070	92	74	GCnPCA	T080-T250	5	109.1	11.6	288.2	12.8	4.9	C	no
mj073	92	74	GCnPCA	T390-T450	3	235.3	72.4	196.1	5.1	2.3	C	no
mj075	92	74	DirOPCA	T450-T570	5	345.1	-28.9	341.9	42.2	11.5	B	no
mj077	92	74	DirOPCA	T330-T420	4	193.5	46.7	190.8	-26.4	14	C	no
mj078	92	74	DirOPCA	T250-T570	10	143	9.7	123	-43.6	10.4	B	yes
mj079	93	74	DirOPCA	T450-T590	11	204.5	29.5	207.6	-40	4.8	A	yes
mj080	93	74	DirOPCA	T330-T390	3	208.4	23	216.1	-43.7	10.4	B	yes
mj081	93	72	GCnPCA	T150-T300	4	101.8	18.2	293	2.4	3.9	C	no
mj082	93	72	GCnPCA	T200-T300	3	106.8	3.6	280.8	11.9	12.6	C	no
mj083	93	72	DirOPCA	T480-T570	8	191	9.4	199.8	-61.5	6.1	A	yes
mj084	93	72	DirOPCA	T360-T575	14	157.9	2.8	130.6	-57.7	14.1	B	yes

mj086	93	72	DirOPCA	T330-T535	10	107.3	60	153.6	-8.6	13.8	C	no
mj087	93	72	GCnPCA	T120-T250	4	113.9	13.2	292.6	15.1	11	C	no
mj088	93	72	DirOPCA	T390-T600	14	205.2	16.6	216.6	-49.1	14.4	B	yes
mj089	93	72	Dir PCA	T480-T570	8	220.8	9.2	240.1	-43.8	8.8	B	yes
mj090	93	72	GCnPCA	T100-T360	7	135.9	36.3	324.1	19.8	3.1	C	no
mj091	93	72	DirOPCA	T330-T530	9	326.2	-3.6	300.1	47.8	5.8	B	no
mj097	93	72	DirOPCA	T420-T510	4	115.4	32.3	130.9	-8.1	5.5	C	no
mj098	93	72	Dir PCA	T360-T450	4	151	12	134.3	-46.4	11.7	B	yes
mj099	93	72	Dir PCA	T330-T420	4	178.9	65.2	181.3	-6.8	10.4	C	no
mj100	93	72	DirOPCA	T360-T450	4	174.8	40.8	175.8	-30.7	10.7	A	yes
mj102	93	72	DirOPCA	T360-T450	4	162.1	21.4	154.7	-45.6	11.4	B	yes
mj103	93	72	Dir PCA	T360-T420	3	158.8	58.2	170.3	-11.2	12.2	B	yes
mj105	93	72	GCnPCA	T120-T250	4	150.7	48.5	341.2	17.5	1.2	C	no
mj106	93	72	Dir PCA	T360-T420	3	168.3	67.8	177.5	-3.5	21.5	C	no
mj107	93	72	DirOPCA	T450-T550	6	181.4	14	180.1	-58	13.9	B	yes
mj108	93	72	DirOPCA	T330-T510	7	153.4	40.3	158.3	-25.6	8.6	B	yes

mj109	93	72	DirOPCA	T200-T300	3	150.1	49.8	161.6	-16.2	8.8	B	yes
mj110	93	72	GCnPCA	T200-T330	4	239	57.7	209.3	2.2	13	C	no
mj111	93	72	DirOPCA	T360-T510	6	183.7	75.9	183.2	-3.9	8.6	B	yes
mj112	93	68	GCnPCA	T560-T580	4	119.8	48.8	147	0.4	6.9	C	no
mj113	93	68	DirOPCA	T540-T590	7	4	-53.9	3.6	14.1	9.3	A	no
mj114	93	68	GCnPCA	T120-T250	4	91.1	13.2	104.6	6.6	4.2	C	no
mj117	93	68	DirOPCA	T560-T600	6	207.3	3.9	228.5	-54.8	0.8	A	yes
mj118	93	68	DirOPCA	T250-T565	14	191.3	-3.8	208	-70.2	7.6	B	yes
mj119	93	68	Dir PCA	T300-T450	6	157.1	-4.3	124.5	-59.3	12.3	B	yes
mj120	93	68	GCnPCA	T300-T360	3	174.8	74.5	180.8	6.6	7.4	C	no
mj122	93	68	DirOPCA	T570-T590	3	106.5	29.3	125	-0.3	1.7	C	no
mj125	93	68	GCnPCA	T200-T300	3	145	39.3	332.7	19.2	5.5	C	no
mj229	288	56	DirOPCA	T390-T600	14	110.3	-24.7	130	-11.7	3.4	A	yes
mj231	288	56	DirOPCA	T450-T600	8	120.9	-24.7	135.5	-3.8	1.4	A	yes
mj232	288	56	DirOPCA	T420-T600	13	99.5	-62.3	164.5	-33.5	0.7	A	yes
mj234	288	56	DirOPCA	T550-T590	6	15.6	69.9	17.2	14	7.9	B	no

mj237	288	56	DirOPCA	T420-T570	11	76.5	-49	145.8	-44.9	9.5	A	yes
mj239	333	43	DirOPCA	T360-T530	7	75.8	-51.7	187.4	-80.4	8.1	B	yes
mj240	333	43	DirOPCA	T360-T510	6	100.4	-47	167	-64.8	8.1	B	yes
mj241	333	43	GCnPCA	T150-T420	8	261.3	15.6	274.8	55.1	13.4	C	no
mj242	333	43	GCnPCA	T80-T330	7	123.9	31.2	111.7	5.4	14.3	C	no
mj243-1	333	43	GCnPCA	T150-T360	6	48.7	6.2	225.5	35.3	15.3	C	no
mj243	333	43	DirOPCA	M20-M70	6	298.6	30	331.7	44.4	13.8	B	no
mj244	333	43	GCnPCA	T150-T360	6	250.1	15	255.8	57.5	6.7	C	no
mj245b	333	43	DirOPCA	M020-M090	8	346.4	51.8	19.8	28.5	4.6	B	no
mj246	333	43	DirOPCA	T330-T480	6	113.9	-29.2	147.2	-47.1	7.9	B	yes
mj247-1	333	43	GCnPCA	T150-T330	5	68.6	10.2	249.5	32.6	6.4	C	no
mj247	333	43	DirOPCA	M20-M90	8	333.6	36.9	0.5	25.7	5.3	C	no

Note: DirOPCA: best-fitting demagnetization trajectory (forced to the origin); DirPCA: best-fitting demagnetization trajectory; GCnPCA: great-circle fit; N: number of demagnetization steps used to define the ChRM; D_g, I_g: Declination and Inclination in geographic coordinates (before tilt correction); D_s, I_s: Declination and Inclination in stratigraphic coordinates (after tilt correction); $\alpha95_s$: 95% limits confidence in stratigraphic coordinates; Grades *A*,*B* and *C* to the Zijderveld diagram best-fits: *A* for very good to excellent, *B* for OK and seems right but doubtful and *C* for doubtful.

Table S2: Fold test results on ChRM with the summation of cosine (SCOS) value for the structural correction using definition 2 of SCOS

The upper Cuojiangding Group (84.3°E, 29.9°N) N = 69 sites	
	SCOS values
In Situ	22.043
Unfolded	0.178
*95%	9.662
**99%	13.662

*(**): 95%(99%) critical values which must be exceeded for significant correlation.

Table S3: Summary of the Late Cretaceous-Eocene palaeomagnetic results from northern India

Location (°N/°E)	Lithology	Age	n	D_s(°)	I_s(°)	α_{95s} (°)	Palaeolat.	VGP Lat.(°)	VGP Long.(°)	Field test	Reference
29/87	Zongpu Fm. sediments	57 Ma	4	154.0	-5.1	8.4	-2.5±5.3	49.8	309.7	F+	Besse *et al.* (1984)[11]
28.7/86.8	Zongpu Fm. sediments	62-66 Ma	3	162.4	-29.1	6.6	-15.6± 4.0	69.1	312.6	——	Tong *et al.* (2008)[12]
28.3/88.5	Zhongshan Fm. sediments	65-71 Ma	14	4.0	-11.2	8.5	-4.7±4.4	55.8	261.4	F+	Patzelt *et al.* (1996)[3]
28.3/88.5	Jidula Fm. sediments	63-66 Ma	4	178.6	-14.4	7.3	8.3±5.7	69.0	272.4	F+	Patzelt *et al.* (1996)[3]
28.3/88.5	Zongpu Fm. sediments	59-63 Ma	14	176.2	-7.9	7.5	5.0±5.9	65.4	277.6	F+	Patzelt *et al.* (1996) [3]
28.3/88.5	Zongpu Fm. sediments	59-62 Ma	18	180.8	-11.1	4.2	6.6±3.5	67.3	266.3	F+, R+	Yi *et al.* (2011)[4]
28.3/88.5	Zongpu Fm. sediments	56-59 Ma	14	177.0	-19.6	3.5	11.1±2.5	71.6	277.8	F+, R+	Yi *et al.* (2011)[4]

Note: n, number of sites; D_s, declination (stratigraphic coordinate); I_s, inclination (stratigraphic coordinate); α_{95}, 95% confidence limit (for stratigraphic data); Palaeolat., palaeolatitude for a reference position; VGP, virtual geomagnetic pole; lat., latitude; long., longitude; Field test, F+, positive fold test, R+, positive reverse test, — no information; Fm., Formation;

Table S4: Summary of the Late Cretaceous-Eocene palaeomagnetic results from southern Tibet

Location (°N/°E)	Lithology	Age	n	D_s(°)	I_s(°)	α_{95s}(°)	Palaeo-lat.	VGP Lat.(°)	VGP Long.(°)	Field test	Reference
					Late Cretaceous Data						
29.4/91.09	Takena Fm. sediments	K_2	7	338.0	36.0	10.0	20.0± 7.8	68.0	340.0	F+	Pozzi and Westphal (1982)[13]
32.0/91.5 North	Takena Fm. sediments	100-125 Ma	6	338.7	25.4	8.9	13.3± 5.0	63.5	325.4	F+	Achache *et al*. (1984)[14]
29.9/91.0 South	Takena Fm. sediments	100-125 Ma	8	354.3	22.6	8.3	11.8± 6.2	71.2	288.4	F+	Achache *et al*. (1984)[14]
29.9/91.2	Takena Fm. sediments	K_2	8	357.0	15.0	6.7	7.6± 3.5	68.0	279.0	F+	Lin and Watts (1988)[15]
29.9/91.2	Shexing Fm. sediments	65-110 Ma	43	350.2	42.0	2.5	24.2± 1.4	79.6	329.9	F+	Tan *et al*. (2010)[5]
29.9/91.2	Shexing Fm. Intercalated Volcanics	85-110 Ma	21	22.6	41.9	4.4	24.2± 3.3	69.1	191.7	F+	Tan *et al*. (2010)[5]
29.9/90.7	Shexing Fm. sediments	72-110 Ma	17	344.1	34.5	5.2	19.0± 5.3	71.9	327.2	F+	Sun *et al*. (2012)[6]
29.9/90.7	Shexing Fm. sediments	72-110 Ma	15	343.4	41.6	2.8	23.8± 2.3	74.1	342.7	F+	van Hinsberg-en *et al*. (2012)[7]
					Palaeogene Data						
29.9/90.0	Linzizong Gp. Volcanics	48.5 Ma	2	0.0	18.0	——	8.3	69.3	271.0	——	Westphal and Pozzi (1983)[16]

29.9/90.0	Linzizong Gp. Volcanics	45-60 Ma	8	170.9	-25.5	11.0	13.5± 6.5	71.5	300.0	——	Achache *et al.* (1984)[14]
29.9/91.2 29.8/89.2	Linzizong Gp. Volcanics+Sedime-nts	60-64 Ma	15	173.5	-14.8	8.8	6.6± 8.5	66	284.9	F+	Chen *et al.* (2010)[17]
30.0/91.2 29.8/89.2	Linzizong Gp. Volcanics+Sedime-nts	44-60 Ma	23	355.9	20.0	6.9	10.8± 5.3	70.6	281.0	F+	Chen *et al.* (2010)[17]
30.0/91.1	Linzizong Gp. Volcanics	47-54 Ma	24	12.5	39.4	5.6	22.3± 5.0	76.9	205.8	——	Dupont-Nivet *et al.* (2010)[18]
29.9/90.0 30.0/91.1 29.9/91.2	Linzizong Gp. Volcanics	40-60 Ma	37	7.7	40.3	5.6	23.0± 4.2	80.8	217.3	F+	Dupont-Nivet *et al.* (2010)*[18]
29.9/91.1	Linzizong Gp. Dykes Volcanics	53 Ma	10	15.4	27.2	9.7	14.4± 5.8	68.9	225.4	F+, R+	Liebke *et al.* (2010)[19]
30.1/90.9	Linzizong Gp. Volcanics	55 Ma	14	359.0	21.6	9.2	13.6± 5.4	73.6	274.3	F+	Sun *et al.* (2010)[20]
29.9/91.2	Linzizong Gp. Volcanics	40-43 Ma	10	359.5	51.8	5.6	32.4± 4.8	86.3	91.2	F+	Tan *et al.* (2010)[5]
——	Linzizong Gp. Volcanics	47-56 Ma	52	3.5	35.5	3.6	19.6± 3.9	80.1	248.6	F+, R+	van Hinsberg-en *et al.* (2012)[7]
29.9/84.3	Upper Cuojiangding Gp. Sediments	54-57 Ma	62	168.1	-42.0	7.1	24.2± 5.9	78.0	329.0	F+	This study
33/88	Volcanics	32-38 Ma	20	——	——	——	28.7	——	——	——	Lippert *et al.* (2011)[10]

Note: n, number of sites; D_s, declination (stratigraphic coordinate); I_s, inclination (stratigraphic coordinate); α_{95}, 95% confidence limit (for stratigraphic data); Palaeolat., palaeolatitude for a reference position; VGP, virtual geomagnetic pole; lat., latitude; long., longitude; Field test, F+, positive fold test, R+, positive reverse test, — no information; Fm., Formation; Gp., Group; Dupont-Nivet *et al.* (2010)*, combined data from Achache *et al.* (1984)[14], Dupont-Nivet *et al.* (2010)[18] and Tan *et al.* (2010)[5].

Table S5: Palaeomagnetic poles and palaeolatitudes for the margin of Asia and India used in Figure 6a

Numbers In Figure 6	Location		Age	Pole Latitude (°N)	Pole Longitude (°E)	Palaeolatitude (°) At Reference Position (29.9°N, 84.3°E)	Reference
	Locality	°N/°E					
	Sothern Asian Margin						
1	Xigaze forearc basin	29.9/84.3	54-57 Ma	78.0	329.0	24.2±5.9	This study
2	Southern Qiangtang terrane	33/88	32-38 Ma	--	--	25.6±3.8	van Hinsbergen *et al*. (2012)[7]
3	Southern Lhasa terrane	29.9/91.2	65-110 Ma	79.6	329.9	25.2±1.4	Tan *et al*. (2010)[5]
4	Southern Lhasa terrane	29.9/90.7	72-110 Ma	74.1	342.7	25.6±2.3	van Hinsbergen *et al*. (2012)[7]
5	Southern Lhasa terrane	29.9/91.2	85-110 Ma	69.1	191.7	21.9±3.3	Tan *et al.* (2010)[5]
	Northern Indian Margin						
6	Tethyan Himalaya	28.3/88.5	65-71 Ma	55.8	261.4	-4.3±4.4	Patzelt *et al.* (1996)[3]
7	Tethyan Himalaya	28.3/88.5	59-62 Ma	67.3	266.3	7.2±3.5	Yi *et al.* (2011)[4]
8	Tethyan Himalaya	28.3/88.5	56-59 Ma	71.6	277.8	11.9±2.5	Yi *et al.* (2011)[4]
	Southern Margin of Eurasian from Apparent Polar Wander Path (APWP)						
9	Eurasian APWP	--	0 Ma	88.5	173.9	29.9±1.9	Torsvik *et al.* (2012)[21]
9	Eurasian APWP	--	10 Ma	86.7	150	31.2±1.8	Torsvik *et al.* (2012)[21]
9	Eurasian APWP	--	20 Ma	84.4	152.1	31.9±2.6	Torsvik *et al.* (2012)[21]
9	Eurasian APWP	--	30 Ma	83.1	146.5	32.9±2.6	Torsvik *et al.* (2012)[21]
9	Eurasian APWP	--	40 Ma	81.1	144.3	33.7±2.9	Torsvik *et al.* (2012)[21]

9	Eurasian APWP	--	50 Ma	78.9	164.7	31.1±2.8	Torsvik *et al.* (2012)[21]
9	Eurasian APWP	--	60 Ma	78.2	172.6	29.6±2.1	Torsvik *et al.* (2012)[21]
9	Eurasian APWP	--	70 Ma	79.2	175.7	29.1±2.5	Torsvik *et al.* (2012)[21]
9	Eurasian APWP	--	80 Ma	79.7	177.9	28.7±2.9	Torsvik *et al.* (2012)[21]
9	Eurasian APWP	--	90 Ma	80.4	167.2	30.6±2.5	Torsvik *et al.* (2012)[21]
9	Eurasian APWP	--	100 Ma	80.8	152.3	33.0±3.3	Torsvik *et al.* (2012)[21]
9	Eurasian APWP	--	110 Ma	81.2	193.1	26.7±3.3	Torsvik *et al.* (2012)[21]
Northern Margin of India from APWP							
10	Indian APWP	--	0 Ma	88.5	173.9	29.9±1.9	Torsvik *et al.* (2012)[21]
10	Indian APWP	--	10 Ma	87.2	240.4	27.3±1.8	Torsvik *et al.* (2012)[21]
10	Indian APWP	--	20 Ma	83.7	254.7	23.7±2.6	Torsvik *et al.* (2012)[21]
10	Indian APWP	--	30 Ma	79.7	281.7	20.0±2.6	Torsvik *et al.* (2012)[21]
10	Indian APWP	--	40 Ma	74.7	286.8	15.6±2.9	Torsvik *et al.* (2012)[21]
10	Indian APWP	--	50 Ma	65.1	278.4	5.6±2.8	Torsvik *et al.* (2012)[21]
10	Indian APWP	--	60 Ma	48.5	280.8	-10.2±2.1	Torsvik *et al.* (2012)[21]
10	Indian APWP	--	70 Ma	36.4	280.7	-21.9±2.5	Torsvik *et al.* (2012)[21]

References for Supplementary Materials:

S1 Day, R., Fuller, M. & Schmidt, V. Hysteresis properties of titanomagnetites: grain-size and compositional dependence. *Phys. Earth Planet In.* **13**, 260-267 (1977).

S2 Dunlop, D. J. Theory and application of the Day plot (Mrs/Ms versus Hcr/Hc) 1. Theoretical curves and tests using titanomagnetite data. *J. geophys. Res.* **107**, B32056 (2002).

S3 Patzelt, A., Li, H. M., Wang, J. D. & Appel, E. Palaeomagnetism of Cretaceous to Tertiary sediments from southern Tibet: Evidence for the extent of the northern margin of India prior to the collision with Eurasia. *Tectonophysics* **259**, 259-284 (1996).

S4 Yi, Z., Huang, B., Chen, J., Chen, L. & Wang, H. Palaeomagnetism of early Palaeogene marine sediments in southern Tibet, China: Implications to onset of the India-Asia collision and size of Greater India. *Earth Planet Sci. Lett.* **309**, 153-165 (2011).

S5 Tan, X. D. *et al.* New palaeomagnetic results from the Lhasa block: Revised estimation of latitudinal shortening across Tibet and implications for dating the India-Asia collision. *Earth Planet Sci. Lett.* **293**, 396-404 (2010).

S6 Sun, Z. *et al.* Palaeomagnetism of late Cretaceous sediments from southern Tibet: Evidence for the consistent palaeolatitudes of the southern margin of Eurasia prior to the collision with India. *Gondwana Res.* **21**, 53-63 (2012).

S7 van Hinsbergen, D. J. J. *et al.* Greater India Basin hypothesis and a two-stage Cenozoic collision between India and Asia. *Proc. Natl Acad. Sci. USA* **109**, 7659-7664 (2012).

S8 Coe, R. S., Globerman, B. R., Plumley, P. W. & Thrupp, G.A. Palaeomagnetic results from Alaska and their tectonic implications. in *Tectonostratigraphic terranes of the Circum-Pacific region: American Association of Petroleum Geologists* (ed D.G. Howell) 85-108 (Circum-Pacific Council on Energy and Resources Earth Sciences Series, 1985).

S9 DeCelles, P. G., Kapp, P., Ding, L. & Gehrels, G. E. Late Cretaceous to middle Tertiary basin evolution in the central Tibetan Plateau: Changing environments in response to tectonic partitioning, aridification, and regional elevation gain. *Geol. Soc. Am. Bull.* **119**, 654-680 (2007).

S10 Lippert, P. C., Zhao, X., Coe, R. S. & Lo, C. H. Palaeomagnetism and 40Ar/39Ar geochronology of upper Palaeogene volcanic rocks from Central Tibet: implications for the Central Asia inclination anomaly, the palaeolatitude of Tibet and post-50 Ma shortening within Asia. *Geophys J. Int.* **184**, 131-161 (2011).

S11 Besse, J., Courtillot, V., Pozzi, J., Westphal, M. & Zhou, Y. Palaeomagnetic estimates of crustal shortening in the Himalayan thrusts and Zangbo suture. *Nature* **311**, 621–626 (1984).

S12 Tong, Y. *et al.* Early Paleocene paleomagnetic results from southern Tibet, and tectonic implications. *Int. Geol. Rev.* **50**, 546-562 (2008).

S13 Pozzi, J. P., Westphal, M., Zhou, Y. X., Xing, L. S. & Chen, X. Y. Position of the Lhasa block, South Tibet, during the late Cretaceous. *Nature* **297**, 319-321 (1982).

S14 Achache, J., Courtillot, V. & Xiu, Z. Y. Palaeogeographic and tectonic evolution of southern Tibet since middle Cretaceous time: New palaeomagnetic data and synthesis. *J. Geophys. Res.* **89**, 10311-10339 (1984)

S15 Lin, J. L. & Watts, D. R. Palaeomagnetic results from the Tibetan Plateau. *Phil. Trans. R. Soc. A, Mathematical and Physical Sciences* **327**, 239-262 (1988).

S16 Westphal, M., Pozzi, J. P., Zhou, Y. X., Xing, L. S. & Chen, X. Y. Palaeomagnetic data about southern Tibet (Xizang)—The Cretaceous formations of the Lhasa block. *Geophysical Journal of the Royal Astronomical Society* **73**, 507-521 (1983).

S17 Chen, J. S., Huang, B. C. & Sun, L. S. New constraints to the onset of the India-Asia collision: Paleomagnetic reconnaissance on the

Linzizong Group in the Lhasa Block, China. *Tectonophysics* **489**, 189-209 (2010).

S18 Dupont-Nivet, G., Lippert, P. C., van Hinsbergen, D. J. J., Meijers, M. J. M. & Kapp, P. Palaeolatitude and age of the Indo-Asia collision: palaeomagnetic constraints. *Geophys J. Int.* **182**, 1189-1198 (2010).

S19 Liebke, U. *et al.* Position of the Lhasa terrane prior to India-Asia collision derived from palaeomagnetic inclinations of 53 Ma old dykes of the Linzhou Basin: constraints on the age of collision and post-collisional shortening within the Tibetan Plateau. *Geophys J. Int.* **182**, 1199-1215 (2010).

S20 Sun, Z. M., Jiang, W., Li, H. B., Pei, J. L. & Zhu, Z. M. New paleomagnetic results of Paleocene volcanic rocks from the Lhasa block: Tectonic implications for the collision of India and Asia. *Tectonophysics* **490**, 257-266 (2010).

S21 Torsvik, T. H. *et al.* Phanerozoic polar wander, palaeogeography and dynamics. *Earth-Sci. Rev.* **114**, 325–368 (2012).